

Exact mobility line and mobility ring in the complex energy plane of a flat band lattice with a non-Hermitian quasiperiodic potential

Guang-Xin Pang,¹ Zhi Li,^{2,3} Shan-Zhong Li,^{2,3} Yan-Yang Zhang,¹ Jun-Feng Liu,¹ and Yi-Cai Zhang^{1,*}

¹*School of Physics and Materials Science, Guangzhou University, Guangzhou 510006, China*

²*Key Laboratory of Atomic and Subatomic Structure and Quantum Control (Ministry of Education), Guangdong Basic Research Center of Excellence for Structure and Fundamental Interactions of Matter, School of Physics, South China Normal University, Guangzhou 510006, China*

³*Guangdong Provincial Key Laboratory of Quantum Engineering and Quantum Materials, Guangdong-Hong Kong Joint Laboratory of Quantum Matter, Frontier Research Institute for Physics, South China Normal University, Guangzhou 510006, China*
(Dated: April 15, 2025)

In this study, we investigate the problem of Anderson localization in a one-dimensional flat band lattice with a non-Hermitian quasiperiodic on-site potential. First of all, we discuss the influences of non-Hermitian potentials on the existence of critical states. Our findings show that, unlike in Hermitian cases, the non-Hermiticity of the potential leads to the disappearance of critical states and critical regions. Furthermore, we are able to accurately determine the Lyapunov exponents and the mobility edges. Our results reveal that the mobility edges form mobility lines and mobility rings in the complex energy plane. Within the mobility rings, the eigenstates are extended, while the localized states are located outside the mobility rings. For mobility line cases, only when the eigenenergies lie on the mobility lines, their corresponding eigenstates are extended states. Finally, as the energy approaches the mobility edges, we observe that, differently from Hermitian cases, here the critical index of the localization length is not a constant, but rather varies depending on the positions of the mobility edges.

I. INTRODUCTION

It is believed that even a weakly uncorrelated disorder in one and two dimensions [1] can lead to Anderson localization [2]. In three dimensional disorder system, there is a mobility edge E_c that separates localized states from delocalized states [3]. Near localized-delocalized transition points (E_c), the localization length $\xi(E)$ diverges, i.e.,

$$\xi(E) \propto |E - E_c|^{-\nu} \rightarrow \infty, \text{ as } E \rightarrow E_c, \quad (1)$$

where ν is the critical index [4]. Interestingly, if the disorder is correlated, the one-dimensional system can have extended states [5] and undergo a localized-extended transition [6]. Furthermore, the correlation between disorders can even lead to the emergence of mobility edges in one-dimensional lattice models [7].

Later on, the investigations of the localized-delocalized transition and mobility edge have been extended to the cases of quasiperiodic potential [8–24]. A famous example where the localized-extended transition can occur is the Aubry-André lattice model (AA model) [8]. However, this system does not have mobility edges. The nonexistence of mobility edges originates from the exact self-duality of this model at the critical point. In general, the breaking of the self-duality would result in the appearance of mobility edges in the one dimension system [25–34].

Ganeshan, Pixley and Das Sarma proposed a generalized Aubry-André model (GAA model) which has mobility edges [35, 36]. The GAA model is

$$t[\psi(n+2) + \psi(n-2)] + \frac{2\lambda \cos(2\pi\beta n + \phi)}{1 - \alpha \cos(2\pi\beta n + \phi)}\psi(n) = E\psi(n). \quad (2)$$

where t is hopping, $n \in \mathbb{Z}$ is lattice site index, λ describes the quasi-periodic potential strength, β is an irrational number, ϕ is a phase, α is a real number. Importantly, its mobility edges can be exactly determined by a generalized self-duality transformation [36]. A mosaic lattice model with quasiperiodic disorder has been proposed [37]. This model has been found to have mobility edges, which can be exactly determined using Avila's theory [38–40].

When $|\alpha| < 1$, the quasi-periodic potential is bounded [see Eq.(2)], and the system can undergo a localized-extended transition. However, when $|\alpha| \geq 1$, the potential is unbounded, resulting in an unbounded energy spectrum. In this case, the system exhibits critical states and undergoes localized-critical transitions [41]. Additionally, there is a critical region in the parameter plane that consists of critical states. As the energy approaches the localized-critical transition point (named as the anomalous mobility edge [42]), the critical index of the localized length is $\nu = 1/2$, which is different from the $\nu = 1$ observed in the bounded case ($|\alpha| < 1$) [41].

Recently, a flat band lattice model was proposed [43], which has much richer physics compared to the original Ganeshan-Pixley-Das Sarma's GAA model. It was found that the physics of localization for both the bounded

* Contact author: E-mail:zhangyicai123456@163.com

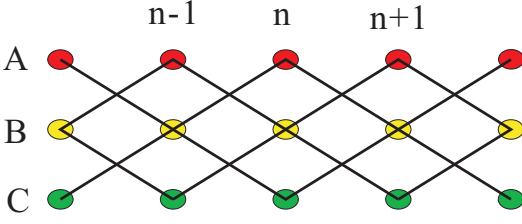


FIG. 1. The figure shows a one-dimensional flat band lattice, composed of two intersecting diamond lattices. The solid lines represent the hopping between lattice sites. The sublattice indices are denoted by A, B, C , and the unit cell indices are represented by $n-1, n, n+1$.

and unbounded quasi-periodic potentials can be realized in this flat band lattice model. Not only can localized states, extended states, and critical states coexist, but the system also exhibits multiple transitions between these states, such as localized-extended, localized-critical, extended-critical, and localized-localized transitions.

The studies of Anderson localization in quasi periodic potentials have been extended to non-Hermitian situations [44–67]. In a non-Hermitian quasiperiodic system, the concept of mobility edge has been generalized to the complex energy plane [68–72], named as a mobility ring [69]. However, exactly analytical results on complex mobility edges are relatively scarce, particularly in non-Hermitian quasiperiodic flat bands. Therefore, it is necessary to extend the study of mobility edges in flat bands to the complex plane in order to explore their physical properties.

One may wonder what would happen if we generalize the above flat model to the non-Hermitian case. What would be the fate of critical states and critical regions under the influences of non-Hermitian potentials? Are there any mobility rings?

In this study, we aim to address the aforementioned questions by expanding upon the flat model to include non-Hermitian quasiperiodic potentials. Our findings reveal that the presence of a non-Hermitian on-site potential results in the disappearances of critical states and critical regions. We provide a thorough explanation for this observation and its underlying mechanism. In such scenarios, the system only exhibits extended and localized states. Compared to localized states, the spatial extensions of extended states are significantly larger.

Additionally, we accurately determine the Lyapunov exponent $\gamma(E)$ using Avila’s theory. This allows us to precisely map out the phase diagram in the complex energy plane and identify mobility edges. Interestingly, we observe that these mobility edges can form not only ring structures, but also line segment structures, which we refer to as mobility lines. Finally, we note that the critical index of localized length in the complex energy plane is dependent on the positions of the mobility edges.

The work is organized as follows. First, the flat band

model and its three energy bands are given in Sec. II. Next, we investigate the localization problem of quasi-periodic potential of “type III” and “type II” in Sec. III and Sec. IV. Finally, a summary is given in Sec. V.

II. THE FLAT BAND MODEL

In this work, like reference [43], we consider the following flat band lattice model consisting of three sublattices A, B , and C , i.e.,

$$H = H_0 + V$$

$$H_0 = -\frac{it}{\sqrt{2}} \sum_{n \in \mathbb{Z}} [a_{n-1}^\dagger b_n + b_{n-1}^\dagger a_n + b_{n-1}^\dagger c_n + c_{n-1}^\dagger b_n] + h.c.$$

$$+ m \sum_{n \in \mathbb{Z}} [a_n^\dagger a_n - c_n^\dagger c_n], \quad (3)$$

where V_p is potential energy, integer n is the unit cell’s index, H_0 is the free-particle Hamiltonian, $t > 0$ is hopping parameter, and $m > 0$ is energy gap parameter. $a(b/c)_n$ are the annihilation operators for the states in sublattices $A(B/C)$, respectively. The flat band lattice structure is depicted in Fig. 1. It is composed of two intersecting diamond lattices, as shown in the figure.

When potential $V_p = 0$, applying a Fourier transform, the free particle Hamiltonian H_0 can be written as

$$H_0 = \sqrt{2}t \sum_{-\pi \leq k \leq \pi} \sin(kd) [a_k^\dagger b_k + b_k^\dagger a_k + b_k^\dagger c_k + c_k^\dagger b_k]$$

$$+ m \sum_{-\pi \leq k \leq \pi} [a_k^\dagger a_k - c_k^\dagger c_k], \quad (4)$$

where d is lattice constant. In the whole manuscript, we would set $d = 1$ for simplifications.

Furthermore, in the above Hamiltonian H_0 , we can identify the above three sublattices A, B, C as three internal spin components 1, 2, 3. After diagonalizing H_0 , we can obtain the three eigenenergies:

$$E_{-,k} = -\sqrt{4t^2 \sin^2(k) + m^2};$$

$$E_{0,k} = 0;$$

$$E_{+,k} = \sqrt{4t^2 \sin^2(k) + m^2}, \quad (5)$$

where $|-(0/+), k\rangle$ denote the eigenstates of lower, middle (flat) and upper bands, respectively. We can see that a flat band with zero energy ($E_{0,k} = 0$) appears between the upper and lower bands.

In the vicinity of momentum $k = 0$, the three-band Hamiltonian described above can be approximated by a continuous spin-1 Dirac model. The bound state problems of this continuous spin-1 Hamiltonian have been extensively studied with various types of potentials [73–77]. It is found that a short-ranged potential can induce an infinite number of bound states, and the bound state in continuum (BIC) can appear.

III. ANDERSON LOCALIZATION IN A NON-HERMITIAN QUASIPERIODIC POTENTIAL OF TYPE III

In the following, we assume the potential energy V_p has following form in basis $|1, 2, 3\rangle$, namely,

$$V_p = \sum_n V_{11}(n) a_n^\dagger a_n. \quad (6)$$

In the whole manuscript, we would refer to such a kind of potential as potential of “type III” [76]. The bound state problems with potential of “type I, II and III” were investigated [73, 75–77].

In this work, we take a specific non-Hermitian quasi-periodic potential, namely

$$V_{11}(n) = V_0 e^{i\theta} \cos(2\pi\beta n + \phi + i\epsilon). \quad (7)$$

where real number V_0 is potential strength, β is a irrational number, θ , ϵ and ϕ are real number. In comparison with Hermitian case [43], here the non-Hermiticity enter into system through the overall phase factor $e^{i\theta}$ and imaginary phase $i\epsilon$ in the cos function. In the following, we take $m = t$, $\beta = \frac{\sqrt{5}-1}{2}$ for the sake of definiteness, and use the units of system of $t = 1$.

Using three component wave functions ψ_1, ψ_2, ψ_3 , the Schrödinger equation ($H|\Psi\rangle = E|\Psi\rangle$) can be expressed by

$$\begin{aligned} \frac{-it}{\sqrt{2}}[\psi_2(n+1) - \psi_2(n-1)] &= [E - m - V_{11}(n)]\psi_1(n), \\ \frac{-it}{\sqrt{2}}[\psi_1(n+1) - \psi_1(n-1) + \psi_3(n+1) - \psi_3(n-1)] \\ &= E\psi_2(n), \\ \frac{-it}{\sqrt{2}}[\psi_2(n+1) - \psi_2(n-1)] &= [E + m]\psi_3(n). \end{aligned} \quad (8)$$

Eliminating wave functions of second and third components in Eq.(8), we get an effective equation for $\psi_1(n)$, i.e.,

$$\begin{aligned} t^2 \left[\frac{E - V_{11}(n+2)/2}{E + m} \psi_1(n+2) - 2 \frac{E - V_{11}(n)/2}{E + m} \psi_1(n) \right. \\ \left. + \frac{E - V_{11}(n-2)/2}{E + m} \psi_1(n-2) \right] \\ = -E[E - m - V_{11}(n)]\psi_1(n). \end{aligned} \quad (9)$$

Further we introduce an auxiliary wave function $\psi(n) \equiv \frac{E - V_{11}(n)/2}{E + m} \psi_1(n)$, an effective hopping \tilde{t} , an effective total energy \tilde{E} , an effective potential strength λ and an effective parameter α , i.e.,

$$\begin{aligned} \tilde{t} &\equiv t^2, \\ \tilde{E} &\equiv -E^2 + m^2 + 2\tilde{t} = -E^2 + m^2 + 2t^2, \\ \lambda &\equiv -\frac{V_0 e^{i\theta} (E + m)^2}{4E}, \\ \alpha &\equiv \frac{V_0 e^{i\theta}}{2E}, \end{aligned} \quad (10)$$

we get an equation for $\psi(n)$

$$\begin{aligned} \tilde{t}[\psi(n+2) + \psi(n-2)] + \frac{2\lambda \cos(2\pi\beta n + \phi + i\epsilon)}{1 - \alpha \cos(2\pi\beta n + \phi + i\epsilon)} \psi(n) \\ = \tilde{E} \psi(n). \end{aligned} \quad (11)$$

Comparing with Eq.(2), it is found that this is an effective generalized Aubry-André model whose effective lattice constant is two times of the original lattice constant, i.e., $\tilde{d} = 2d = 2$.

From Eq. (10), we can see that when $\theta = 0$ and E is real, the effective parameter α is also real. Further, when $\epsilon = 0$ and the effective parameter $|\alpha| \geq 1$, the effective potential $\frac{2\lambda \cos(2\pi\beta n + \phi + i\epsilon)}{1 - \alpha \cos(2\pi\beta n + \phi + i\epsilon)} = \frac{2\lambda \cos(2\pi\beta n + \phi)}{1 - \alpha \cos(2\pi\beta n + \phi)}$ in Eq.(11) becomes unbounded. In the previous studies [41, 43], it is found that the unbounded potential would lead to critical states, critical regions, and localized-critical transitions.

However, in the presence of non-Hermitian conditions where $\theta \neq 0$ or $\epsilon \neq 0$, the critical states and critical regions disappear, leaving only localized and extended states. This can be explained as follows: the wave function of an extended state typically spans the entire lattice, while a localized state occupies only a finite number of lattice sites. The critical state is composed of several disconnected patches that interpolate between the localized and extended states [41–43, 78, 79]. As a result, the wave function of a critical state usually takes a value of zero at the lattice site where it is disconnected. This is due to the unboundedness of the quasiperiodic potential. When $|\alpha| \geq 1$, the denominator of the potential, $|1 - \alpha \cos(2\pi\beta n + \phi)|$, can become arbitrarily small at some lattice sites due to the ergodicity of the map $\phi \rightarrow \phi + 2\pi\beta$. This means that for a given eigenenergy $E = E_n$, the potential $\frac{2\lambda \cos(2\pi\beta n + \phi)}{1 - \alpha \cos(2\pi\beta n + \phi)}$ can take arbitrarily large values at these sites. As a result, the wave function becomes vanishingly small and disconnected at these lattice sites, leading to the appearance of critical states.

From these discussions, we can understand that the reason for the occurrence of critical states is that as lattice site index n varies, the denominator of the quasiperiodic potential can approach zero. Roughly speaking, in the case of an unbounded Hermitian potential, the denominator can become zero. However, in the case of non-Hermitian conditions where $\theta \neq 0$ or $\epsilon \neq 0$, the denominator of the potential $1 - \alpha \cos(2\pi\beta n + \phi + i\epsilon)$ becomes a complex number. In order for the denominator to be zero, both the real and imaginary parts must be zero. However, it is highly unlikely for both the real and imaginary parts to be zero at the same time as lattice site index n varies. Therefore, the critical state is unlikely to occur in this case, and the system will only have localized and extended states.

The localized properties of an eigenstate can be characterized by Lyapunov exponent. For a given parameter E , as n increases, we can assume that the wave function grows exponentially according to a law [80, 81], expressed

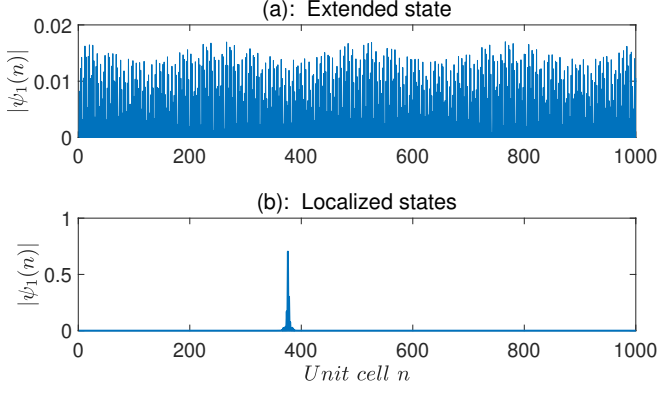


FIG. 2. Two typical wave functions for extended states and localized states.

as

$$\psi(n) \sim e^{\gamma(E)n}, \text{ as } n \rightarrow \infty, \quad (12)$$

where $\gamma(E) \geq 0$ is Lyapunov exponent which measures the average growth rate of wave function. If the parameter E is not an eigen-energy of H , the Lyapunov exponent will be positive, i.e., $\gamma(E) > 0$ [82]. When E is an eigen-energy of the system, the Lyapunov exponent can be either zero or positive [41], depending on the type of state. Extended and critical states have a Lyapunov exponent of zero, while localized states have a positive exponent.

When E belongs to eigenvalues, using Avila's theory [38, 39, 83], we can get the exact expression of Lyapunov exponent, i.e. (for detailed calculation, please refer to the Appendix),

$$\gamma(E, \epsilon) = \begin{cases} \frac{1}{2} \text{Max}\{0, |\epsilon| + \ln\left(\frac{|P \pm \sqrt{P^2 - 4\alpha^2}|}{2|1 + \sqrt{1 - \alpha^2}|}\right)\}, \\ \text{for } |\epsilon| < \ln\left(\frac{1 + \sqrt{1 - \alpha^2}}{\alpha}\right) \\ \frac{1}{2} \text{Max}\{0, \ln\left(\frac{|P \pm \sqrt{P^2 - 4\alpha^2}|}{2|\alpha|}\right)\}, \\ \text{for } |\epsilon| \geq \ln\left(\frac{1 + \sqrt{1 - \alpha^2}}{\alpha}\right) \end{cases} \quad (13)$$

where

$$P = \frac{\alpha \tilde{E} + 2\lambda}{\tilde{t}}. \quad (14)$$

To analyze the properties of the eigenstates, we have utilized numerical methods to solve Eq. (8). Our approach involves using a total of $N = 1000$ unit cells and constructing a $3N \times 3N$ matrix with open boundary conditions at the two end sites. This matrix is then diagonalized, resulting in $3 \times N = 3000$ eigenenergies and eigenstates. Two typical wave functions for extended state and localized state are shown in Fig. (2).

In addition, with Eq.(11), the Lyapunov exponent can be calculated numerically with transfer matrix method, i.e.,

$$\begin{aligned} \gamma(E, \epsilon) &= \lim_{L \rightarrow \infty} \frac{\ln(|\Psi(2L)|/|\Psi(0)|)}{2L} \\ &= \lim_{L \rightarrow \infty} \frac{\ln(|T(2L)T(2L-2)\dots T(4)T(2)\Psi(0)|/|\Psi(0)|)}{2L} \end{aligned} \quad (15)$$

where L is a positive integer, transfer matrix

$$T(n) \equiv \begin{bmatrix} \frac{\tilde{E}}{\tilde{t}} - \frac{2\lambda}{\tilde{t}} \frac{\cos(2\pi\beta n + \phi + i\epsilon)}{1 - \alpha \cos(2\pi\beta n + \phi + i\epsilon)} & -1 \\ 1 & 0 \end{bmatrix}, \quad (16)$$

$$\Psi(n) \equiv \begin{bmatrix} \psi(n+2) \\ \psi(n) \end{bmatrix}, \quad (17)$$

and

$$|\Psi(n)| = \sqrt{|\psi(n+2)|^2 + |\psi(n)|^2}. \quad (18)$$

To be specific, after we obtain the corresponding eigenenergies and eigenstates, we then proceed to numerically calculate the Lyapunov exponents for all of these eigenenergies, as shown by the discrete red squares in Fig. 3. In our numerical calculation, we take $L = 200$, phase $\phi = 0$, $\psi(0) = 0$ and $\psi(2) = 1$ in Eq.(15).

Eq. (13) has been confirmed by our numerical results, as shown in Fig. 3. The blue dots in Fig. 3 are given by Eq. (13) for all the eigenvalues. It is evident that the two sets of discrete points overlap very well on the graph.

In order to distinguish the localized states from the extended states, we numerically calculate standard deviation of coordinates of eigenstates [84], i.e.,

$$\sigma(n) = \sqrt{\sum_{\delta=1,2,3;j} (j - \bar{j})^2 |\psi_{\delta}(j)|^2}, \quad (19)$$

where ψ_{δ} is the n th normalized wave function and the average value of coordinate \bar{j} is

$$\bar{j} = \sum_{\delta=1,2,3;j} j |\psi_{\delta}(j)|^2. \quad (20)$$

The standard deviation σ describes the spatial extension of the wave function in the lattice. In Fig. 4, the standard deviations are represented with different colors of the color bar. The phase diagram in complex energy plane is also shown in Fig. 4. Panel (a) of Fig. 5 shows the standard deviations for all the eigenstates as a function of real parts of eigenenergy E_n . From Fig. 3, 4 and panel (a) of Fig. 5, we can see the black points in Fig. 4 are localized states which have very small standard deviations, while the yellow points are extended states which have much larger standard deviations.

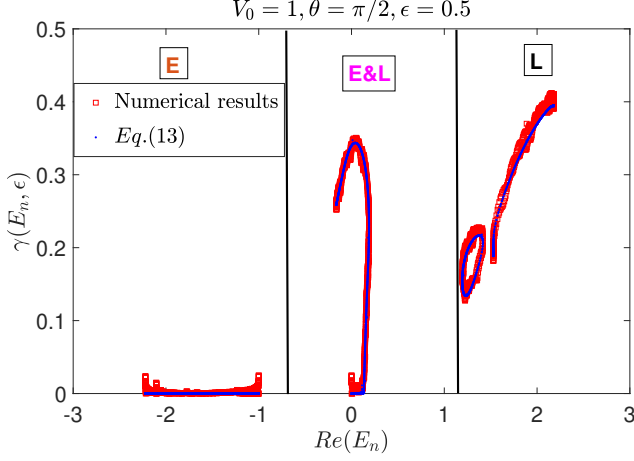


FIG. 3. Lyapunov exponent for quasi-periodic potential of type III with $V_0 = 1, \theta = \pi/2, \epsilon = 0.5$. The red squares represent the results from numerical calculation using Eq.(15), while the blue dots are obtained from Eq.(13). It is evident that the two sets of discrete points overlap very well. Here **L**, **E** and **E & L** denote localized states, extended states and the mixture of localized and extended states, respectively. It is evident that the Lyapunov exponents of localized states are positive, while the Lyapunov exponents for extended states are zero (also see Figs. 4 and 5).

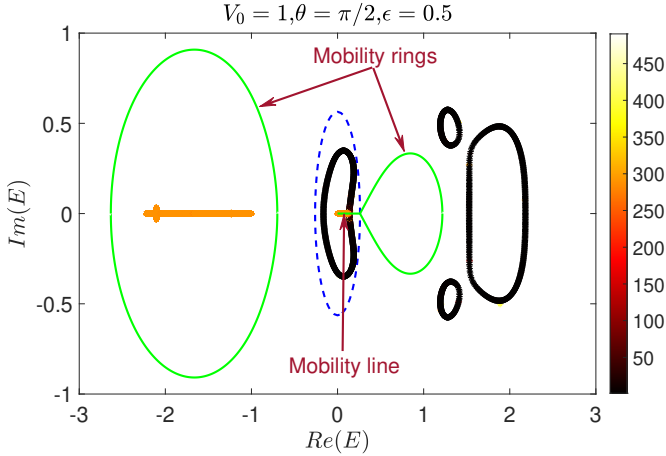


FIG. 4. The phase diagram for quasi-periodic potential of type III in the complex number E plane for $V_0 = 1, \theta = \pi/2, \epsilon = 0.5$ and lattice size $3 \times N = 3 \times 1000 = 3000$. The phase boundaries, also known as mobility edges E_c , are indicated by the green solid line segment and curves, and their equations are given by Eqs. (25) and (31). The states within the green loops and on the green line segment (yellow points) are extended states, while those outside the loops (represented by black points) are localized states. The blue dashed curve is the ellipse given by Eq.(22). Standard deviations are represented by different colors of the color bar.

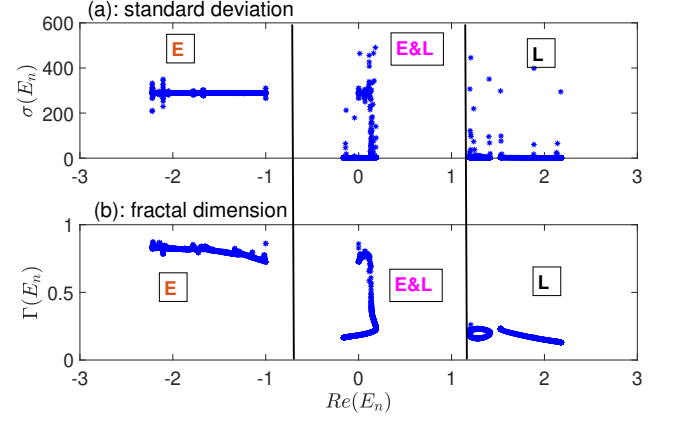


FIG. 5. (a): standard deviation and (b): fractal dimension for quasi-periodic potential of type III with $V_0 = 1, \theta = \pi/2, \epsilon = 0.5$. Here **L**, **E** and **E & L** represent localized states, extended states and the mixture of localized and extended states, respectively.

In order to further investigate the properties of the wave function, we also numerically calculate the fractional dimension of the eigenstate, which is defined by [69, 85, 86], i.e.,

$$\Gamma(n) = -\frac{\ln(\sum_{\delta j} |\psi_{\delta}(j)|^4)}{\ln(N)}. \quad (21)$$

where ψ_{δ} is the n th normalized wave function. From panel (b) of Fig. 5, we see that for localized states, the fractal dimensions are small, while for extended states, the fractal dimensions are larger. So both the standard deviations and fractal dimensions can be used to distinguish the localized from extended states.

IV. MOBILITY LINES AND MOBILITY RINGS IN THE COMPLEX ENERGY PLANE

From Eq. (13), we can see that the two different expressions for the Lyapunov exponent are separated by the equation $|\epsilon| = \ln \left| \frac{1+\sqrt{1-\alpha^2}}{\alpha} \right|$. This equation forms an ellipse in the complex energy plane (please refer to the detailed proof in the Appendix). The equation of the ellipse can be explicitly given by:

$$\frac{(x \cos \theta + y \sin \theta)^2}{\left(\frac{V_0}{2} \cosh \epsilon\right)^2} + \frac{(y \cos \theta - x \sin \theta)^2}{\left(\frac{V_0}{2} \sinh \epsilon\right)^2} = 1, \quad (22)$$

where $x = \text{Re}(E)$ and $y = \text{Im}(E)$. We see that the angle between the major axis of ellipse and positive real axis of E is θ (as shown by the blue dashed curves in Figs. 4 and 6). When $\theta = 0$ and $\epsilon = 0$, this ellipse is reduced to a line segment, given by $-V_0/2 < E < V_0/2$. If E lies on the line segment, the parameter α would satisfies

$|\alpha| = |\frac{V_0}{2E}| > 1$, which defines the unbounded Hermitian cases [43]. While for general non-Hermitian cases, this ellipse divides the entire complex energy plane into two parts.

A. mobility lines inside the ellipse

$$\frac{(x \cos \theta + y \sin \theta)^2}{(\frac{V_0}{2} \cosh \epsilon)^2} + \frac{(y \cos \theta - x \sin \theta)^2}{(\frac{V_0}{2} \sinh \epsilon)^2} < 1$$

By Eq.(13), we find that inside the ellipse, the Lyapunov exponent is given by

$$\gamma(E, \epsilon) = \frac{1}{2} \text{Max}\{0, \ln(\frac{|P \pm \sqrt{P^2 - 4\alpha^2}|}{2|\alpha|})\}. \quad (23)$$

Then the mobility edges, denoted by E_c which separates the localized states from the extended states, can be determined as follows:

$$\frac{1}{2} \text{Max}\{0, \ln(\frac{|P \pm \sqrt{P^2 - 4\alpha^2}|}{2|\alpha|})\} = 0. \quad (24)$$

By Eq.(24), then we find

$$E_c \in [-2, -1] \cup [0, 1]. \quad (25)$$

We observe that Eq.(25) is independent of the phase θ and $i\epsilon$. To be precise, here the mobility edges are determined by the intersection of two sets: $\{E = x + yi | \frac{(x \cos \theta + y \sin \theta)^2}{(\frac{V_0}{2} \cosh \epsilon)^2} + \frac{(y \cos \theta - x \sin \theta)^2}{(\frac{V_0}{2} \sinh \epsilon)^2} < 1\}$ and $\{E | E \in [-2, -1] \cup [0, 1]\}$, which are represented by the green solid line segments inside the blue dashed ellipses in Figs. 4 and 6.

Furthermore, it has been observed that within the ellipse, if imaginary part of E_n is not zero [$\text{Im}(E_n) \neq 0$], the Lyapunov exponent is always positive, indicating localized states (represented by the black points inside the blue dashed ellipses in Figs. 4 and 6). Only when $E_n = E_c$, these states become extended (represented by the yellow points on the green line segments in Figs. 4 and 6). This implies that only when the eigenenergies lie on the mobility lines, their corresponding eigenstates are extended states.

By expanding the Lyapunov exponent [Eq.(13)] near the mobility edges E_c (the points on the green line segments in Figs. 4 and 6), we can determine the behavior of Lyapunov, i.e.,

$$\gamma(E, \epsilon) \propto |E - E_c|^\nu \rightarrow 0, \text{ as } E \rightarrow E_c. \quad (26)$$

Then the localization length is

$$\xi(E) \equiv 1/\gamma(E, \epsilon) \propto |E - E_c|^{-\nu} \rightarrow \infty, \text{ as } E \rightarrow E_c, \quad (27)$$

where ν is the critical index of localized length. We find that the critical index ν depends on the position of E_c .

For example, if $E_c = 0$, when E approaches $E_c = 0$, the critical index $\nu = 1/2$, i.e.,

$$\xi(E) \propto |E - E_c|^{-1/2} \rightarrow 0, \text{ as } E \rightarrow E_c = 0. \quad (28)$$

While when E approaches $E_c = 1/3$, the critical index $\nu = 1$, i.e.,

$$\xi(E) \propto |E - E_c|^{-1} \rightarrow 0, \text{ as } E \rightarrow E_c = 1/3. \quad (29)$$

This shows that, differently from Hermitian cases [41], here the critical index ν is not a constant, but rather varies depending on the positions of mobility edges in the complex energy plane.

B. mobility rings outside the ellipse

$$\frac{(x \cos \theta + y \sin \theta)^2}{(\frac{V_0}{2} \cosh \epsilon)^2} + \frac{(y \cos \theta - x \sin \theta)^2}{(\frac{V_0}{2} \sinh \epsilon)^2} > 1$$

When the energy is outside the ellipse, by Eq.(13), the Lyapunov exponent is given by

$$\gamma(E, \epsilon) = \frac{1}{2} \text{Max}\{0, |\epsilon| + \ln(\frac{|P \pm \sqrt{P^2 - 4\alpha^2}|}{2|1 + \sqrt{1 - \alpha^2}|})\}. \quad (30)$$

Then the mobility edges, denoted by E_c , can be determined as follows:

$$\frac{1}{2} \text{Max}\{0, |\epsilon| + \ln(\frac{|P \pm \sqrt{P^2 - 4\alpha^2}|}{2|1 + \sqrt{1 - \alpha^2}|})\} = 0. \quad (31)$$

It is found that the mobility edges form closed loops in complex energy plane, named as mobility rings [69] which are represented by the green solid curves in Fig. 4 and 6.

When the eigenvalues are outside the mobility rings, their Lyapunov exponents are always positive, then these states corresponds localized states (see black points outside the blue ellipses in Figs. 4 and 6). Only when eigenvalues are inside the mobility rings, their Lyapunov exponents are zero, and the states correspond extended states (see yellow points outside the blue ellipses in Figs. 4 and 6).

C. mobility rings in quasi-periodic potential of Type II

In this subsection, for the sake of completeness, we investigate the Anderson localization problem in the flat band lattice model for a non-Hermitian quasi-periodic potential of Type II. We assume that the potential energy, denoted as V_p , takes the following form in the spin basis $|1, 2, 3\rangle$:

$$V_p = \sum_n V_{22}(n) b_n^\dagger b_n. \quad (32)$$

Note that the potential only appears in the basis element $|2\rangle$ (or sublattice B). Throughout the manuscript, we will refer to this type of potential as ‘‘type II’’ potential [73].

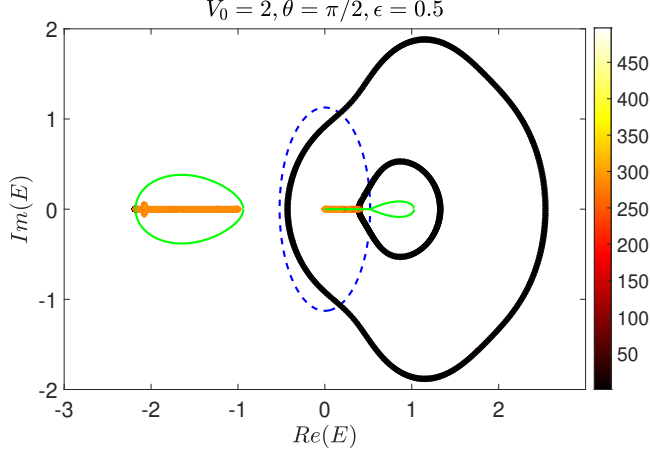


FIG. 6. The phase diagram for quasi-periodic potential of type III in the complex E plane for $V_0 = 2, \theta = \pi/2, \epsilon = 0.5$ and lattice size $3N = 3 \times 1000 = 3000$. The phase boundaries (mobility edges E_c) are indicated by the green solid line segment and curves, and their equations are given by Eqs. (25) and (31). These states which are within the green loops and on the green line segment (yellow color points) are extended states, while those outside the loops are localized states (black color points). The blue dashed curve is the ellipse given by Eq.(22).

Furthermore, like $V_{11}(n)$, we assume $V_{22}(n)$ is also a non-Hermitian quasi-periodical potential, i.e.,

$$V_{22}(n) = V_0 e^{i\theta} \cos(2\pi\beta n + \phi + i\epsilon). \quad (33)$$

The Schrödinger equation can be written as

$$\begin{aligned} -it[\psi_2(n+1) - \psi_2(n-1)]/\sqrt{2} &= [E - m]\psi_1(n), \\ -it[\psi_1(n+1) - \psi_1(n-1) + \psi_3(n+1) - \psi_3(n-1)]/\sqrt{2} &= [E - V_{22}(n)]\psi_2(n), \\ -it[\psi_2(n+1) - \psi_2(n-1)]/\sqrt{2} &= [E + m]\psi_3(n). \end{aligned} \quad (34)$$

Eliminating wave functions for first and third components, we get an effective Schrödinger equation for ψ_2

$$\begin{aligned} -t^2[\psi_2(n+2) - 2\psi_2(n) + \psi_2(n-2)] \\ + \frac{(E^2 - m^2)V_{22}(n)}{E}\psi_2(n) &= [E^2 - m^2]\psi_2(n). \end{aligned} \quad (35)$$

Further introducing an effective hopping \tilde{t} , an effective energy \tilde{E} and an effective potential strength λ

$$\begin{aligned} \tilde{t} &\equiv t^2, \\ \tilde{E} &\equiv -E^2 + m^2 + 2t^2, \\ \lambda &\equiv V_0 e^{i\theta} (-E^2 + m^2)/(2E), \end{aligned} \quad (36)$$

Eq.(35) becomes a non-Hermitian Aubry-André (AA) model, i.e.,

$$\begin{aligned} \tilde{t}[\psi_2(n+2) + \psi_2(n-2)] + 2\lambda \cos(2\pi\beta n + \phi + i\epsilon)\psi_2(n) \\ = \tilde{E}\psi_2(n). \end{aligned} \quad (37)$$

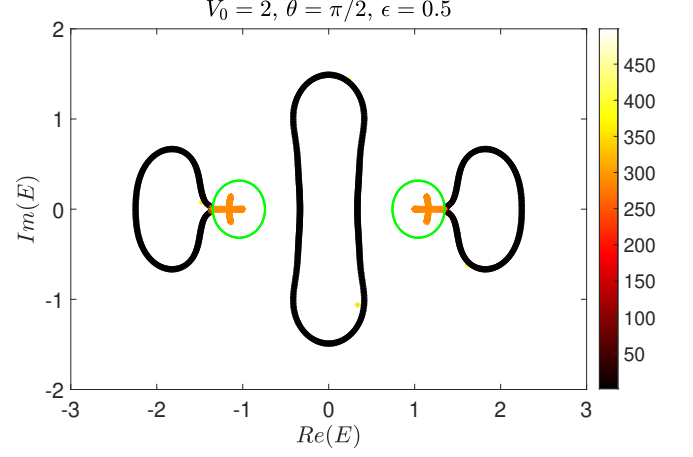


FIG. 7. Phase diagram for quasi-periodic potential of type II with $V_0 = 2, \theta = \pi/2, \epsilon = 0.5$. The phase boundaries (mobility edges E_c) are indicated by the green solid curves, and their equations are given by Eq. (39). The states which are inside the green rings (yellow color points) are extended states, while those outside the rings are localized states (black color points). The standard deviations are represented by different colors of the color bar.

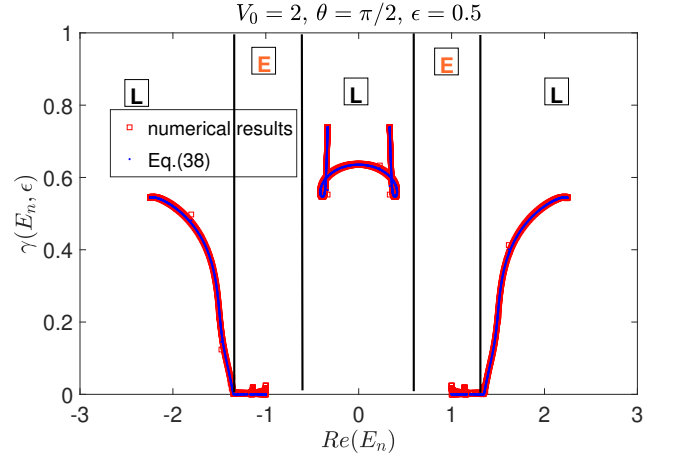


FIG. 8. Lyapunov exponent for quasi-periodic potential of type II with $V_0 = 2, \theta = \pi/2, \epsilon = 0.5$. The red squares are obtained through numerical calculation, while the blue dots are obtained using Eq.(38). It is evident that the two sets of discrete points overlap perfectly. Here **L** and **E** represent localized states, extended states, respectively.

Using Avila's theory, the Lyapunov exponent for the AA model is given by (see the Appendix)

$$\begin{aligned} \gamma(E, \epsilon) &= \frac{1}{2} \text{Max}\{0, |\epsilon| + \ln(|\frac{\lambda}{\tilde{t}}|)\} \\ &= \frac{1}{2} \text{Max}\{0, |\epsilon| + \ln(|\frac{V_0(E^2 - m^2)}{2Et^2}|)\}. \end{aligned} \quad (38)$$

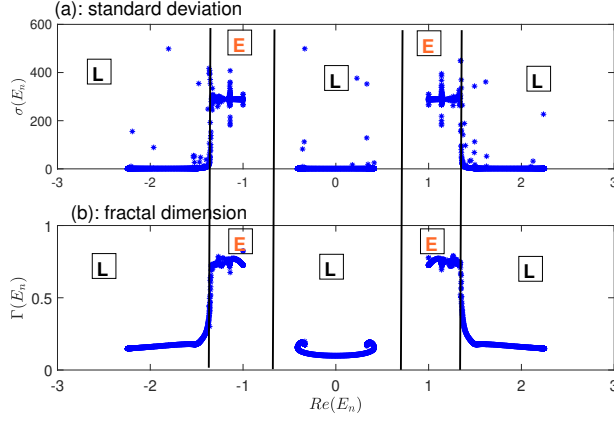


FIG. 9. (a): standard deviation and (b):fractal dimension for quasi-periodic potential of type II with $V_0 = 2, \theta = \pi/2, \epsilon = 0.5$. Here **L** and **E** represent localized states, extended states, respectively.

By Eq.(38), the mobility edges are determined by

$$\begin{aligned} \gamma(E_c) &= \frac{1}{2} \text{Max}\{0, |\epsilon| + \ln(|\frac{\lambda}{t}|)\} = 0, \\ \Rightarrow |\epsilon| + \ln(|\frac{\lambda}{t}|) &= 0, \\ \Rightarrow (x - \frac{x}{x^2 + y^2})^2 + (y + \frac{y}{x^2 + y^2})^2 &= \frac{4t^4 e^{-2|\epsilon|}}{m^2 V_0^2}, \quad (39) \end{aligned}$$

where $x = \text{Re}(E_c)/m$ and $y = \text{Im}(E_c)/m$. The mobility edges form mobility rings in the complex energy plane, represented by the green solid curves in Fig. 7. The phase diagram is also presented in Fig. 7, and the different colors of color bar represent different values of the standard deviations.

According to Eq. (39), the mobility rings are not affected by the parameter θ . As the absolute value of ϵ increases, the sizes of the mobility rings decrease. In particular, when $|\epsilon| \rightarrow \infty$, the mobility rings shrink into two points and disappear eventually.

Using transfer matrix method, we also performed numerical calculations for the Lyapunov exponents (represented by the set of red squares in Fig. 8). The blue dots in Fig. 8 represent the values obtained from Eq. (38) for all eigenenergies. The perfect overlap of the two sets of discrete points indicates a strong agreement between the analytical and numerical results.

We also calculated the standard deviations and fractal dimensions for all the eigenstates. The results are shown in Fig. 9. From Fig. 9, it is evident that the standard deviations and fractal dimensions are significantly smaller for localized states compared to extended states.

V. SUMMARY

In conclusion, we investigate the localization properties of a one-dimensional flat band lattice model with a non-Hermitian quasiperiodic on-site potential. Our findings indicate that the presence of a non-Hermitian potential leads to the disappearance of critical states and critical regions. By utilizing Avila's theory, we determine the exact Lyapunov exponents and mobility edges. Our results show that the mobility edges not only form mobility rings, but also mobility lines in the complex energy plane. Within the mobility rings, the states are extended, while the states outside the rings are localized. For mobility line cases, only when the eigenenergies lie on these lines, their corresponding eigenstates are extended states. Furthermore, our research suggests that the critical index of the localization length can vary depending on the positions of mobility edges in the complex energy plane.

ACKNOWLEDGEMENTS

This work was supported by the NSFC under Grants Nos. 11874127, 12074180, 12174077, Guangdong Basic and Applied Basic Research Foundation under No. 2023A1515010698, the Joint Fund with Guangzhou Municipality under No.202201020137, and the Starting Research Fund from Guangzhou University under Grant No. RQ 2020083.

APPENDIX

A. derivations of Eq.(13) and Eq.(38)

In this subsection of Appendix, we use the transfer matrix method [87, 88] to calculate the Lyapunov exponent. First of all, let us assume that the system [Eq.(11)] is a half-infinite lattice with left-hand end sites at $n = 0$ and $n = 2$. Further using Eq.(11), starting with $\psi(0)$ and $\psi(2)$ of left-hand end sites, we can calculate the wave function for the entire system [41], i.e.,

$$\Psi(2L) = T(2L)T(2L-2)...T(4)T(2)\Psi(0) \quad (40)$$

where transfer matrix

$$T(n) \equiv \begin{bmatrix} \frac{\tilde{E}}{t} - \frac{2\lambda}{t} \frac{\cos(2\pi\beta n + \phi + i\epsilon)}{1 - \alpha \cos(2\pi\beta n + \phi + i\epsilon)} & -1 \\ 1 & 0 \end{bmatrix}, \quad (41)$$

and

$$\Psi(n) \equiv \begin{bmatrix} \psi(n+2) \\ \psi(n) \end{bmatrix}. \quad (42)$$

The Lyapunov exponent is defined by

$$\begin{aligned}\gamma(E, \epsilon) &= \lim_{L \rightarrow \infty} \frac{\ln(|\Psi(2L)|/|\Psi(0)|)}{2L} \\ &= \lim_{L \rightarrow \infty} \frac{\ln(|T(2L)T(2L-2)\dots T(4)T(2)\Psi(0)|/|\Psi(0)|)}{2L}\end{aligned}\quad (43)$$

where L is a positive integer, and the modulus is defined as

$$|\Psi(n)| = \sqrt{|\psi(n+2)|^2 + |\psi(n)|^2}. \quad (44)$$

The transfer matrix Eq.(41) can be further written as a product of two parts, i.e., $T_n = A_n B_n$, where

$$\begin{aligned}A_n &= \frac{1}{1 - \alpha \cos(2\pi\beta n + \phi + i\epsilon)}, \\ B_n &= \begin{bmatrix} B_{11} & B_{12} \\ B_{21} & 0 \end{bmatrix},\end{aligned}\quad (45)$$

with $B_{11} = \frac{\tilde{E}}{t}[1 - \alpha \cos(2\pi\beta n + \phi + i\epsilon)] - 2\lambda \cos(2\pi\beta n + \phi + i\epsilon)/\tilde{t}$, and $B_{21} = -B_{12} = 1 - \alpha \cos(2\pi\beta n + \phi + i\epsilon)$.

Now the Lyapunov exponent can be written as

$$\gamma(E, \epsilon) = \gamma_A(E, \epsilon) + \gamma_B(E, \epsilon), \quad (46)$$

where

$$\gamma_A(E, \epsilon) = \lim_{L \rightarrow \infty} \frac{\ln(|A(2L)A(2L-2)\dots A(4)A(2)|)}{2L}, \quad (47)$$

and $\gamma_B(E)$ are given by

$$\begin{aligned}\gamma_B(E, \epsilon) &= \lim_{L \rightarrow \infty} \frac{\ln(|B(2L)B(2L-2)\dots B(4)B(2)\Psi(0)|/|\Psi(0)|)}{2L}.\end{aligned}\quad (48)$$

In the following, we will utilize Avila's theory [38] to obtain the Lyapunov exponent. First of all, the ergodicity of the map $\phi \rightarrow 2\pi\beta n + \phi$ allows us write $\gamma_A(E)$ as an integral over phase ϕ [39, 89, 90], consequently

$$\begin{aligned}\gamma_A(E, \epsilon) &= \frac{1}{2 \times 2\pi} \int_0^{2\pi} d\phi \ln\left(\left|\frac{1}{1 - \alpha \cos(\phi + i\epsilon)}\right|\right) \\ &= \begin{cases} -\frac{1}{2} \ln\left(\left|\frac{1+\sqrt{1-\alpha^2}}{2}\right|\right), \\ \text{for } |\epsilon| < \ln\left(\left|\frac{1+\sqrt{1-\alpha^2}}{\alpha}\right|\right) \\ -\frac{|\epsilon|}{2} - \frac{1}{2} \ln\left(\frac{|\alpha|}{2}\right), \\ \text{for } |\epsilon| \geq \ln\left(\left|\frac{1+\sqrt{1-\alpha^2}}{\alpha}\right|\right) \end{cases}\end{aligned}\quad (49)$$

Note: in contrast to the Hermitian case [41, 43], here α is a complex number in general [see Eq. (10)]. In

the calculation of the above integral, we utilize Jensen's formula for a complex variable function, which is related to the zeros, the poles and the value of the origin of the complex variable function [91, 92].

Next we take $|\epsilon| \rightarrow +\infty$, then

$$B_n = \frac{e^{-i \operatorname{sgn}(\epsilon)(2\pi\beta n + \phi) + |\epsilon|}}{2} \begin{bmatrix} \frac{-(\alpha\tilde{E} + 2\lambda)}{\tilde{t}} & \alpha \\ -\alpha & 0 \end{bmatrix} + O(1), \quad (50)$$

where $\operatorname{sgn}(\epsilon)$ is the sign function of ϵ . Then for large $|\epsilon|$, i.e., $|\epsilon| \gg 1$, $\gamma_B(E, \epsilon)$ is determined by the largest eigenvalue (in absolute value) of B_n , i.e.,

$$\gamma_B(E, \epsilon) = \frac{|\epsilon|}{2} + \frac{1}{2} \operatorname{Max}\left\{\ln\left(\frac{|P \pm \sqrt{P^2 - 4\alpha^2}|}{4}\right)\right\}, \quad (51)$$

where

$$P = \frac{\alpha\tilde{E} + 2\lambda}{\tilde{t}}. \quad (52)$$

Using the facts that $\gamma(E, \epsilon) \geq 0$ and $\gamma(E, \epsilon)$ is piecewise linear function of ϵ [38], one can get

$$\gamma(E, \epsilon) = \operatorname{Max}\{0, \gamma_A(E, \epsilon) + \gamma_B(E, \epsilon)\},$$

$$= \begin{cases} \frac{1}{2} \operatorname{Max}\{0, |\epsilon| + \ln\left(\frac{|P \pm \sqrt{P^2 - 4\alpha^2}|}{2|1 + \sqrt{1 - \alpha^2}|}\right)\}, \\ \text{for } |\epsilon| < \ln\left(\left|\frac{1 + \sqrt{1 - \alpha^2}}{\alpha}\right|\right) \\ \frac{1}{2} \operatorname{Max}\{0, \ln\left(\frac{|P \pm \sqrt{P^2 - 4\alpha^2}|}{2|\alpha|}\right)\}, \\ \text{for } |\epsilon| \geq \ln\left(\left|\frac{1 + \sqrt{1 - \alpha^2}}{\alpha}\right|\right) \end{cases} \quad (53)$$

which is Eq. (13) in main text.

When α approaches 0, i.e. $\alpha \rightarrow 0$, Eq. (11) becomes formally equivalent to Eq. (37). According to Eq. (52), P approaches $2\lambda/\tilde{t}$, and for any arbitrary ϵ , the inequality $|\epsilon| < \ln\left(\left|\frac{1 + \sqrt{1 - \alpha^2}}{\alpha}\right|\right) \rightarrow +\infty$ always holds. Therefore, Eq. (53) can be simplified to Eq. (38) in the main text. This means that we can view Eq. (38) as a special case of Eq. (53).

It is important to note that although the two definitions of effective λ in Eq. (10) and Eq. (36) are different, the derivation of the Lyapunov exponent only depends on the function form of the quasiperiodic potential, rather than the specific value of λ . Therefore, the arguments presented above are still valid.

B. The proof of $|\epsilon| = \ln\left(\left|\frac{1 + \sqrt{1 - \alpha^2}}{\alpha}\right|\right)$ is an ellipse

From the definition of α Eq. (10), let us set

$$\alpha = \frac{V_0 e^{i\theta}}{2E} \equiv \frac{1}{z} \Rightarrow z = \frac{2e^{-i\theta}E}{V_0}, \quad (54)$$

and then the equation becomes

$$|\epsilon| = \ln\left(\left|\frac{1 + \sqrt{1 - \alpha^2}}{\alpha}\right|\right) \Rightarrow |z + \sqrt{z^2 - 1}| = e^{|\epsilon|}. \quad (55)$$

Next we represent complex number z as $z = x + yi$ where x and y are real and imaginary parts of z , respectively. Then, the above equation is

$$|z + \sqrt{z^2 - 1}| = |x + yi + \sqrt{x^2 - y^2 - 1 + 2xyi}| = e^{|\epsilon|}. \quad (56)$$

Further we write $x^2 - y^2 - 1 + 2xyi$ as a square of a complex number $m + ni$, i.e.,

$$x^2 - y^2 - 1 + 2xyi = (m + ni)^2, \quad (57)$$

where m, n are two real number, then we get

$$\begin{aligned} |z + \sqrt{z^2 - 1}| &= |x + yi + \sqrt{x^2 - y^2 - 1 + 2xyi}| \\ &= |x + yi + m + ni| = e^{|\epsilon|}. \end{aligned} \quad (58)$$

So we get

$$(x + m)^2 + (y + n)^2 = e^{2|\epsilon|}. \quad (59)$$

By Eq. (57), we have

$$\begin{aligned} x^2 - y^2 - 1 &= m^2 - n^2, \\ xy &= mn. \end{aligned} \quad (60)$$

Solving Eq. (60), we get

$$\begin{aligned} m &= \frac{\sqrt{-1 + x^2 - y^2 + \sqrt{1 - 2x^2 + x^4 + 2y^2 + 2x^2y^2 + y^4}}}{\sqrt{2}}, \\ n &= \frac{xy}{m}. \end{aligned} \quad (61)$$

Further we assume $m = kx$ and $n = y/k$ where k is a real number to be determined. We find that Eq. (61) becomes an equation of ellipse:

$$(1 - k^2)x^2 + \left(\frac{1}{k^2} - 1\right)y^2 = 1. \quad (62)$$

and Eq. (59) is also an equation of ellipse, i.e.,

$$(1 + k)^2x^2 + (1 + 1/k)^2y^2 = e^{2|\epsilon|}. \quad (63)$$

These above two equations should lead to a same ellipse, then comparing Eq. (62) with Eq. (63), we find

$$(1 + k)^2e^{-2|\epsilon|} = 1 - k^2 \Rightarrow k = \tanh(|\epsilon|), \quad (64)$$

then

$$\begin{aligned} 1 - k^2 &= \frac{1}{\cosh^2(\epsilon)}, \\ \frac{1}{k^2} - 1 &= \frac{1}{\sinh^2(\epsilon)}. \end{aligned} \quad (65)$$

So the ellipse Eq. (62) is

$$\frac{x^2}{\cosh^2(\epsilon)} + \frac{y^2}{\sinh^2(\epsilon)} = 1. \quad (66)$$

From Eq. (54), we have

$$\begin{aligned} z &= \frac{2e^{-i\theta}E}{V_0} \Rightarrow x + yi \\ &= \frac{2}{V_0}\{Re(E)\cos\theta + Im(E)\sin\theta \\ &\quad + i[-Re(E)\sin\theta + Im(E)\cos\theta]\}, \end{aligned} \quad (67)$$

where complex energy $E = Re(E) + iIm(E)$. Then

$$\begin{aligned} x &= \frac{2}{V_0}[Re(E)\cos\theta + Im(E)\sin\theta], \\ y &= \frac{2}{V_0}[(-Re(E)\sin\theta + Im(E)\cos\theta)]. \end{aligned} \quad (68)$$

Substituting Eq. (68) into Eq. (66), the equation of ellipse becomes

$$\frac{[Re(E)\cos\theta + Im(E)\sin\theta]^2}{\left(\frac{V_0}{2}\cosh\epsilon\right)^2} + \frac{[Im(E)\cos\theta - Re(E)\sin\theta]^2}{\left(\frac{V_0}{2}\sinh\epsilon\right)^2} = 1. \quad (69)$$

Finally if we reset $Re(E) \equiv x$ and $Im(E) \equiv y$ in Eq. (69), then we get the equation of the ellipse

$$\frac{(x\cos\theta + y\sin\theta)^2}{\left(\frac{V_0}{2}\cosh\epsilon\right)^2} + \frac{(y\cos\theta - x\sin\theta)^2}{\left(\frac{V_0}{2}\sinh\epsilon\right)^2} = 1, \quad (70)$$

where $E = x + yi$.

-
- [1] E. N. Economou, *Green's Functions in Quantum Physics*, (Springer-Verlag Berlin Heidelberg, Third Edition, 2006).
[2] P. W. Anderson, Absence of Diffusion in Certain Random Lattices, *Phys. Rev.* **109**, 1492 (1957).
[3] E. N. Economou and Morrel H. Cohen, Existence of Mobility Edges in Anderson's Model for Random Lattices,

- Phys. Rev.* **5**, 2931 (1972).
[4] Bodo Huckestein and Bernhard Kramer, One-Parameter Scaling in the Lowest Landau Band: Precise Determination of the Critical Behavior of the Localization Length, *Phys. Rev. Lett.* **64**, 1437 (1990).
[5] Wei Zhang and Sergio E. Ulloa, Extended states in disordered systems: Role of off-diagonal correlations, *Phys.*

- Rev. B **69**, 153203 (2004).
- [6] H. Cheraghchi, S. M. Fazeli, and K. Esfarjani, Localization-delocalization transition in a one-dimensional system with long-range correlated off-diagonal disorder, Phys. Rev. B **72**, 174207 (2005).
 - [7] J C Flores, Transport in models with correlated diagonal and off-diagonal disorder, J. Phys.: Condens. Matter **1**, 8471 (1989).
 - [8] Aubry, S. & Andre, G. Analyticity breaking and anderson localization in incommensurate lattices. Ann. Isr. Phys. Soc **3**, 18 (1980).
 - [9] D. J. Thouless, Localization by a potential with slowly varying period, Phys. Rev. Lett. **61**, 2141 (1988).
 - [10] M. Kohmoto, Metal-insulator transition and scaling for incommensurate systems, Phys. Rev. Lett. **51**, 1198 (1983).
 - [11] M. Kohmoto and D. Tobe, Localization problem in a quasiperiodic system with spin-orbit interaction, Phys. Rev. B **77**, 134204 (2008).
 - [12] X. Cai, L.-J. Lang, S. Chen, and Y. Wang, Topological superconductor to Anderson localization transition in one dimensional incommensurate lattices, Phys. Rev. Lett. **110**, 176403 (2013).
 - [13] G. Roati, C. D Errico, L. Fallani, M. Fattori, C. Fort, M. Zaccanti, G. Modugno, M. Modugno, and M. Inguscio, Anderson localization of a non-interacting Bose-Einstein condensate, Nature (London) **453**, 895 (2008).
 - [14] Y. Lahini, R. Pugatch, F. Pozzi, M. Sorel, R. Morandotti, N. Davidson, and Y. Silberberg, Observation of a localization transition in quasiperiodic photonic lattices, Phys. Rev. Lett. **103**, 013901 (2009).
 - [15] X. Deng, S. Ray, S. Sinha, G. V. Shlyapnikov, and L. Santos, One-dimensional quasicrystals with power-law hopping, Phys. Rev. Lett. **123**, 025301 (2019).
 - [16] J. Gao, I. M. Khaymovich, X.-W. Wang, Z.-S. Xu, A. Iovan, G. Krishna, A. V. Balatsky, V. Zwiller, and A. W. Elshaari, Experimental probe of multi-mobility edges in quasiperiodic mosaic lattices, arXiv:2306.10829.
 - [17] M. Goncalves, B. Amorim, E. V. Castro, and P. Ribeiro, Renormalization group theory of one-dimensional quasiperiodic lattice models with commensurate approximants, Phys. Rev. B **108**, L100201 (2023).
 - [18] D. D. Vu and S. Das Sarma, Generic mobility edges in several classes of duality-breaking one-dimensional quasiperiodic potentials, Phys. Rev. B **107**, 224206 (2023).
 - [19] M. Goncalves, B. Amorim, E. V. Castro, and P. Ribeiro, Critical phase dualities in 1D exactly solvable quasiperiodic models, Phys. Rev. Lett. **131**, 186303 (2023).
 - [20] Z. Xu, H. Huangfu, Y. Zhang, and S. Chen, Dynamical observation of mobility edges in one-dimensional incommensurate optical lattices, New J. Phys. **22**, 013036 (2020).
 - [21] X. Li and S. Das Sarma, Mobility edge and intermediate phase in one-dimensional incommensurate lattice potentials, Phys. Rev. B **101**, 064203 (2020).
 - [22] F. A. An, K. Padavić, E. J. Meier, S. Hegde, S. Ganeshan, J. H. Pixley, S. Vishveshwara, and B. Gadway, Interactions and mobility edges: Observing the generalized Aubry-André model, Phys. Rev. Lett. **126**, 040603 (2021).
 - [23] Z. Wang, Y. Zhang, L. Wang, and S. Chen, Engineering mobility in quasiperiodic lattices with exact mobility edges, Phys. Rev. B **108**, 174202 (2023).
 - [24] Xiaoshui Lin, Xiaoman Chen, Guang-Can Guo, and Ming Gong, General approach to the critical phase with coupled quasiperiodic chains, Phys. Rev. B **108**, 174206 (2023).
 - [25] S. D. Sarma, S. He, X. C. Xie, Mobility edge in a model one-dimensional potential. Phys. Rev. Lett. **61**, 2144 (1988).
 - [26] S. D. Sarma, S. He, X. C. Xie, X. Localization, mobility edges, and metal-insulator transition in a class of one-dimensional slowly varying deterministic potentials. Phys. Rev. B **41**, 5544 (1990).
 - [27] Q. Tang, Y. He, Mobility edges in one-dimensional models with quasi-periodic disorder. J. Phys.: Condens. Matter **33**, 185505 (2021).
 - [28] Shreekantha Sil, Santanu K. Maiti, and Arunava Chakrabarti, Metal-insulator transition in an a periodic ladder network: An exact result. Phys. Rev. Lett. **101**, 076803 (2008).
 - [29] Francois Delyon, Barry Simon, and Bernard Souillard, From power-localized to extended states in a class of one-dimensional disordered systems, Phys. Rev. Lett. **52**, 2187(1984).
 - [30] F. M. Izrailev, A. A. Krokhnin, Localization and the mobility edge in one-dimensional potentials with correlated disorder. Phys. Rev. Lett. **82**, 4062 (1999).
 - [31] D. H. Boers, Benjamin Goedeke, M. Holthaus, Mobility edges in bichromatic optical lattices. Phys. Rev. A **75**, 063404 (2007).
 - [32] X. L. Li, S. D. Sarma, Mobility edges in one-dimensional bichromatic incommensurate potentials. Phys. Rev. B **96**, 085119 (2017).
 - [33] H P Lüschen, S Scherg, T Kohlert, M Schreiber, P Bordia, X Li, S Das Sarma, I Bloch, Single-particle mobility edge in a one-dimensional quasiperiodic optical lattice. Phys. Rev. Lett. **120**, 160404 (2018).
 - [34] H Yao, A Khoudli, L Bresque, L Sanchez-Palencia, Critical behavior and fractality in shallow one-dimensional quasi-periodic potentials. Phys. Rev. Lett. **123**, 070405 (2019).
 - [35] J. Biddle and S. Das Sarma, Predicted mobility edges in one-dimensional incommensurate optical lattices an exactly solvable model of anderson localization. Phys. Rev. Lett. **104**, 070601 (2010).
 - [36] Sriram Ganeshan, J.H. Pixley, and S. Das Sarma, Nearest neighbor tight binding models with an exact mobility edge in one dimension. Phys. Rev. Lett. **114**, 146601 (2015).
 - [37] Yucheng Wang, Xu Xia, Long Zhang, Hepeng Yao, Shu Chen, Jiangong You, Qi Zhou, and Xiong-Jun Liu, One-Dimensional Quasiperiodic Mosaic Lattice with Exact Mobility Edges, Phys. Rev. Lett. **125**, 196604 (2020).
 - [38] Artur Avila, Global theory of one-frequency Schrödinger operators, Acta Math., **215** (2015), 1-54.
 - [39] Yucheng Wang, Xu Xia, Yongjian Wang, Zuohuan Zheng, and Xiong-Jun Liu, Duality between two generalized Aubry-André models with exact mobility edges, Phys. Rev. B **103**, 174205 (2021).
 - [40] X.-C. Zhou, Y. Wang, T.-F. J. Poon, Q. Zhou, and X.-J. Liu, Exact new mobility edges between critical and localized states, Phys. Rev. Lett. **131**, 176401 (2023).
 - [41] Yi-Cai Zhang, and Yan-Yang Zhang, Lyapunov exponent, mobility edges, and critical region in the generalized Aubry-André model with an unbounded quasiperiodic potential, Phys. Rev. B **105**, 174206 (2022).

- [42] T. Liu, X. Xia, S. Longhi, and L. Sanchez-Palencia, Anomalous mobility edges in one-dimensional quasiperiodic models, *SciPost Phys.* **12**, 27 (2022).
- [43] Yi-Cai Zhang, Critical regions in a one-dimensional flat band lattice with a quasi-periodic potential. *Sci Rep* **14**, 17921 (2024).
- [44] A. Jazaeri and I. I. Satija, Localization transition in incommensurate non-Hermitian systems, *Phys. Rev. E* **63**, 036222 (2001).
- [45] H. Jiang, L.-J. Lang, C. Yang, S.-L. Zhu, and S. Chen, Interplay of non-Hermitian skin effects and Anderson localization in nonreciprocal quasiperiodic lattices, *Phys. Rev. B* **100**, 054301(2019).
- [46] Y. Liu, Q. Zhou, and S. Chen, Localization transition, spectrum structure, and winding numbers for one-dimensional non-Hermitian quasicrystals, *Phys. Rev. B* **104**, 024201(2021).
- [47] Y. Liu, X.-P. Jiang, J. Cao, and S. Chen, Non-Hermitian mobility edges in one-dimensional quasicrystals with parity-time symmetry, *Phys. Rev. B* **101**, 174205 (2020).
- [48] S. Schiffer, X.-J. Liu, H. Hu, and J. Wang, Anderson localization transition in a robust PT-symmetric phase of a generalized Aubry-André model, *Phys. Rev. A* **103**, L011302 (2021).
- [49] X. Cai, Localization and topological phase transitions in nonHermitian Aubry-André-Harper models with p-wave pairing, *Phys. Rev. B* **103**, 214202 (2021).
- [50] Y. Liu, Y. Wang, Z. Zheng, and S. Chen, Exact non-Hermitian mobility edges in one-dimensional quasicrystal lattice with exponentially decaying hopping and its dual lattice, *Phys. Rev. B* **103**, 134208 (2021).
- [51] Q.-B. Zeng and Y. Xu, Winding numbers and generalized mobility edges in non-Hermitian systems, *Phys. Rev. Res.* **2**, 033052 (2020).
- [52] C. Yuce and H. Ramezani, Coexistence of extended and localized states in the one-dimensional non-Hermitian Anderson model, *Phys. Rev. B* **106**, 024202 (2022).
- [53] X. Cai, Boundary-dependent self-dualities, winding numbers, and asymmetrical localization in non-Hermitian aperiodic one dimensional models, *Phys. Rev. B* **103**, 014201 (2021).
- [54] S. Longhi, Phase transitions in a non-Hermitian Aubry-André-Harper model, *Phys. Rev. B* **103**, 054203 (2021).
- [55] Z. Xu, X. Xia, and S. Chen, Non-Hermitian Aubry-André model with power-law hopping, *Phys. Rev. B* **104**, 224204(2021).
- [56] W. Han and L. Zhou, Dimerization-induced mobility edges and multiple reentrant localization transitions in non-Hermitian quasicrystals, *Phys. Rev. B* **105**, 054204 (2022).
- [57] T. Liu and X. Xia, Real-complex transition driven by quasiperiodicity: A class of non-PT symmetric models, *Phys. Rev. B* **105**, 054201 (2022).
- [58] W. Chen, S. Cheng, J. Lin, R. Asgari, and G. Xianlong, Breakdown of the correspondence between the real-complex and delocalization-localization transitions in non-Hermitian quasicrystals, *Phys. Rev. B* **106**, 144208 (2022).
- [59] L. Zhou, Non-Abelian generalization of non-Hermitian quasicrystals: PT-symmetry breaking, localization, entanglement, and topological transitions, *Phys. Rev. B* **108**, 014202 (2023).
- [60] X. Xia, K. Huang, S. Wang, and X. Li, Exact mobility edges in the non-Hermitian t1-t2 model: Theory and possible experimental realizations, *Phys. Rev. B* **105**, 014207 (2022).
- [61] S. Gandhi and J. N. Bandyopadhyay, Topological triple phase transition in non-Hermitian quasicrystals with complex asymmetric hopping, *Phys. Rev. B* **108**, 014204 (2023).
- [62] A. Padhan, S. R. Padhi, and T. Mishra, Complete delocalization and reentrant topological transition in a nonHermitian quasiperiodic lattice, *Phys. Rev. B* **109**, L020203 (2024).
- [63] Q. Lin, T. Li, L. Xiao, K. Wang, W. Yi, and P. Xue, Topological phase transitions and mobility edges in non-Hermitian quasicrystals, *Phys. Rev. Lett.* **129**, 113601 (2022).
- [64] L.-Z. Tang, G.-Q. Zhang, L.-F. Zhang, and D.-W. Zhang, Localization and topological transitions in non-Hermitian quasiperiodic lattices, *Phys. Rev. A* **103**, 033325 (2021).
- [65] A. P. Acharya and S. Datta, Localization transitions in a nonHermitian quasiperiodic lattice, *Phys. Rev. B* **109**, 024203 (2024).
- [66] I. D. Vatik, A. Tikan, G. Onishchukov, D. V. Churkin, and A. A. Sukhorukov, Anderson localization in synthetic photonic lattices, *Sci. Rep.* **7**, 4301 (2017).
- [67] Xiang-Ping Jiang, Weilei Zeng, Yayun Hu, Lei Pan, Exact anomalous mobility edges in one-dimensional non-Hermitian quasicrystals, arXiv:2409.03591.
- [68] Tong Liu, Hao Guo, Yong Pu, and Stefano Longhi, Generalized Aubry-Andre self-duality and mobility edges in non-Hermitian quasiperiodic lattices, *Phys. Rev. B* **102**, 024205 (2020).
- [69] Shan-Zhong Li and Zhi Li, Ring structure in the complex plane: A fingerprint of a non-Hermitian mobility edge, *Physical review B* **110**, L041102 (2024).
- [70] L. Wang, J. Liu, Z. Wang, and S. Chen, Exact complex mobility edges and flagellate spectra for nonHermitian quasicrystals with exponential hoppings, arXiv:2406.10769.
- [71] Li Wang, Zhenbo Wang, and Shu Chen, Non-Hermitian butterfly spectra in a family of quasiperiodic lattices, *Physical review B* **110**, L060201 (2024).
- [72] Shan-Zhong Li, Enhong Cheng, Shi-Liang Zhu and Zhi Li, Asymmetric transfer matrix analysis of Lyapunov exponents in one-dimensional nonreciprocal quasicrystals, *Phys. Rev. B* **110**, 134203 (2024)
- [73] Yi-Cai Zhang, Guo-Bao Zhu, Infinite bound states and hydrogen atom-like energy spectrum induced by a flat band. *J. Phys. B: At. Mol. Opt. Phys.* **55**, 065001 (2022).
- [74] A V Zolotaryuk, Y. Z. & Gusynin, V. P. Bound states and point interactions of the one-dimensional pseudospin-one hamiltonian. *J. Phys. A: Math. Theor.* **56**, 485303(2023).
- [75] Yi-Cai Zhang, Wave function collapses and 1/n energy spectrum induced by a coulomb potential in a one-dimensional flat band system. *Chin. Phys. B* **31**, 050311(2022).
- [76] Yi-Cai Zhang, Infinite bound states and 1/n energy spectrum induced by a coulomb potential of type III in a flat band system. *Phys. Scr.* **97**, 015401 (2022).
- [77] Yi-Cai Zhang, Bound states in the continuum (bic) protected by self-sustained potential barriers in a flat band system. *Sci. Reports* **12**, 11670 (2022).
- [78] Yi-Cai Zhang, Rong Yuan, Shuwei Song, Mingpeng Hu, Chaofei Liu, and Yongjian Wang, Odd-even effect of the mosaic modulation period of quasiperiodic hopping on

- the Anderson localization in a one-dimensional lattice model, *Phys. Rev. B* **111**, 064201 (2025).
- [79] Shan-Zhong Li, Yi-Cai Zhang, Yucheng Wang, Shan-chao Zhang, Shi-Liang Zhu, and Zhi Li, Multifractal-enriched mobility edges and emergent quantum phases in one-dimensional exactly solvable lattice models, arXiv:2501.07866.
 - [80] K. Ishii, Localization of eigenstates and transport phenomena in the one-dimensional disordered system, *Progr. Theor. Phys. Suppl.*, **53**: 77 (1973).
 - [81] H. Furstenberg, Noncommuting random products, *Trans. Amer. Math. Soc.*, **108**: 377-428 (1963).
 - [82] R. A. Johnson, Exponential dichotomy, rotation number, and linear differential operators with bounded coefficients, *J. Differential Equations* **61** (1986): 54-78.
 - [83] Yongjian Wang, Xu Xia, Jiangong You, Zuohuan Zheng, and Qi Zhou, Exact mobility edges for 1d quasiperiodic models. arXiv: 2110.00962v1.
 - [84] Dave J. Boers, Benjamin Goedeke, Dennis Hinrichs, and Martin Holthaus, Mobility edges in bichromatic optical lattices, *Phys. Rev. A* **75**, 063404 (2007).
 - [85] Xiaopeng Li, J. H. Pixley, Dong-Ling Deng, Sriram Ganeshan, and S. Das Sarma, Quantum nonergodicity and fermion localization in a system with a single-particle mobility edge, *Phys. Rev. B* **93**, 184204 (2016).
 - [86] Dong-Ling Deng, Sriram Ganeshan, Xiaopeng Li, Ranjan Modak, Subroto Mukerjee, J. H. Pixley, Many-body localization in incommensurate models with a mobility edge, *Annalen der Physik*, **529**, 1600399 (2017).
 - [87] Eugene Sorets and Thomas Spencer, Positive Lyapunov Exponents for Schrödinger Operators with Quasi-Periodic Potentials, *Commun. Math. Phys.* **142**, 543-566 (1991).
 - [88] P. S. Davids, Lyapunov exponent and transfer-matrix spectrum of the random binary alloy, *Phys. Rev. B* **52**, 4146 (1995).
 - [89] Yongjian Wang, Xu Xia, Jiangong You, Zuohuan Zheng, and Qi Zhou, Exact mobility edges for 1D quasiperiodic models, *Communications in Mathematical Physics*, **401**, pages 2521-2567 (2023).
 - [90] Stefano Longhi, Metal-insulator phase transition in a non-Hermitian Aubry-André-Harper model, *Phys. Rev. B* **100**, 125157 (2019).
 - [91] https://en.wikipedia.org/wiki/Jensen's_formula.
 - [92] Lingrui Ge, Svetlana Jitomirskaya, Jiangong You, Qi Zhou, Multiplicative Jensen's formula and quantitative global theory of one-frequency Schrödinger operators, arXiv:2306.16387.